Bank of High-gain Observers in Output Feedback Control: Robustness Analysis Against Measurement Noise

Kasra Esfandiari and Mehran Shakarami

Abstract—This paper analyzes output feedback control of a class of unknown nonlinear systems in the presence of measurement noise using multiple high-gain observers (MHGO). It is well-known that single high-gain observers (HGO) are not able to provide satisfactory performance when the system output is contaminated by noise, and in turn, controllers, which utilize such estimations, perform poorly. To address this issue and improve the control performance, a bank of HGOs is employed, and an appropriate combination of their estimations is used for control purposes. The proposed strategy is capable of mitigating destructive effects of measurement noise and improving transient response, and it does that because it introduces an extra design parameter. The performance recovery capabilities of MHGO-based controllers and the stability of the closed-loop system are discussed. Simulations are performed on an underwater vehicle system and a mechanical system to evaluate the performance of the MHGO-based controller. Furthermore, a detailed comparison to controllers based on conventional HGO, HGO with switching gain, and multi-observer approach is provided, which shows the superiority of the MHGO-based controller over the other methods.

I. INTRODUCTION

STATES of systems have a prominent role in control theory, and many different strategies are developed by using them. Since not all of system state variables are measurable in practice, different observation schemes are presented in the control literature. However, most of previous studies were confined to systems with noise-free output to simplify understudied problems. This assumption is not realistic since measurements are mostly contaminated by noise; not only does this cause unsatisfactory performance, but it may also push the closed-loop system into instability. Hence, it is necessary to investigate the robustness of observers and observer-based controllers [1]. When a priori knowledge exists about the plant and the measurement noise has specific features, Kalman filter is known as a powerful tool for estimation purposes [2]. Several other studies have been also carried out on this field, e.g., see [3]–[6] and references therein. In [3], a fusion estimation algorithm is presented in terms of linear matrix inequalities for a class of uncertain linear systems. This scheme is based on the assumptions that the uncertain part of the plant satisfies certain conditions and multiple sensors measure the output, each of them has its own measurement noise. The problem of speed

observation in mechanical systems is investigated in [4], and a Luenberger-based observer is proposed, capabilities of which in providing promising results in the presence of noise are shown via experiment results. By combining the Kazantzis-Kravaris-Luenberger observer and the parameter estimation-based observer, a state observer design technique is presented for nonlinear systems in [5], and its performance against measurement noise is also discussed by simulations. In [6], an adaptive observer is designed for a class of nonlinear systems with known dynamics and noisy measurements. However, the assumption of availability of a priori knowledge about system dynamics is not always valid. Moreover, the control problem, which is more challenging than the state estimation problem, is remained intact in the works above.

On the other hand, high-gain observers are well-known as powerful structures for state estimation of nonlinear systems. These observers are capable of handling system uncertainties and providing fast and accurate estimations if their gains are chosen sufficiently large [7]. For control purposes, it has been shown that by feeding sufficiently fast HGO-based state estimations into a globally bounded controller, the output feedback controller can recover the performance of the state feedback controller [8]. HGOs, having these nice features, have attracted a great deal of attention in the past few decades and have been widely used in systems and control theory [9]–[12]. However, conventional HGOs with large gains yield state estimations with substantial overshoots/undershoots in the transient response, known as the peaking phenomenon. Such behavior may result in a closed-loop system with a finite escape time, and in turn, might destabilize the overall plant [13].

In addition to the peaking phenomenon, another problem with the conventional HGOs is sensitivity to measurement noise [7]. That is because the basic idea behind the conventional HGOs is to differentiate the system output to get estimations of immeasurable states. Thus, the performance of HGO-based structures should be evaluated with extra attentions since the effects of measurement noise will be greatly amplified by differentiating the system output [14]. The impact of measurement noise on the state estimations of HGOs is discussed in [15], and it has been shown that the gain of observer should not be selected too large or too small. In general, there is a trade-off between measurement noise sensitivity and the convergence rate of state estimation [16]. However, in HGO-based feedback controllers, sufficiently fast reconstruction of system states is a must to assure that an

K. Esfandiari is with the Center for Systems Science, Yale University, New Haven, CT 06511, USA e-mail: (kasra.esfandiari@yale.edu).

M. Shakarami is with the Engineering and Technology Institute Groningen, University of Groningen, 9747 AG Groningen, The Netherlands (e-mail: m.shakarami@rug.nl).

appropriate state estimation is available before the system states leave the region of attraction [13]. In [17] and [18], new HGO structures are proposed for nonlinear systems in the presence of measurement noise. In [17], a large gain is employed, initially, to estimate system states fast; then the observer gain is switched to a smaller value to get a better steady state behavior. Although the basic idea behind this observation strategy is valuable, determining the switching time and the transient peaks may become challenging. In [18], a new structure is presented for HGOs in which the dimension of the observer is $2n - 2$ with a gain that grows up to power 2, where n is the number of state variables. However, the proposed approach does not have any impact on second order systems and the challenging control problem is remained intact there.

Several attempts have been made to incorporate HGOs with adaptive structures. In such observation strategies, intelligent strategies (e.g., fuzzy systems, neural networks, etc.) are employed to estimate the system uncertainties and that approximation is fed into the dynamical equation of the HGO-based structure [19]–[21]. Although such structures may be applicable to a wide class of systems, they do not necessarily provide a nice transient response, specially when the initial conditions are chosen arbitrarily. Because, it takes a relatively long time for the intelligent part to learn the system dynamics, and in turn, these approaches result in an oscillatory response which is an inherent drawback of single adaptive models/structures [22]–[24]. On the other hand, it has been shown that multiple model-based topologies are capable of providing parameter and state estimations with improved transient response [25], [26]. In [27]–[29], the transient response improvement of adaptive systems and observers is performed using the idea of switching between multiple models. Two main drawbacks of the switching based approaches are that a large number of models are needed to guarantee improvement of performance and only information of one model is employed at each time instant. To address the problem of identification of constant parameters in linear systems and avoid from the issues associated with switching schemes, the idea of second level adaptation was proposed in [30].

As motivated above, we will investigate the output feedback control problem of nonlinear systems in the presence of measurement noise. In this regard, a bank of HGOs are utilized for state estimation purposes, which enables us to improve the transient response of conventional HGOs and mitigate destructive effects of measurement noise. The employed observation strategy, MHGO, uses all the information gathered from various observers simultaneously, and a weighted summation of these observations is considered as the final estimation. The main contributions of the paper can be summarized as follows:

- It is shown that there exist some weights enabling us to estimate the system states accurately and to speed up the estimation process in the presence of noise. This re-parameterization introduces an extra design parameter to the problem; hence the need for a large gain, which is required in the conventional HGOs, is mitigated.
- The output feedback control problem in the presence of

measurement noise is addressed, and the stability of the closed-loop system is ensured by using the Lyapunov's direct method.
- It is proven that a separation principle is valid when the state estimations provided by the MHGO are used for control purposes, and the MHGO-based controller is capable of recovering performance of the state feedback controller.
- The robustness analysis of the MHGO-based controller is discussed, and the conditions on the bound of measurement noise and observer gain are derived.

The remainder of this paper is organized as follows: The system equation and the problem under consideration are stated in Section II. Section III includes some preliminaries about convex sets and the HGO as well as the structure of the MHGO and comments on its performance. The key results on robustness analysis of the closed-loop system when the MHGO-based estimations are fed into a controller are presented in Section IV. Section V provides simulation results for the proposed approach and comparisons with the existing methods. Finally Section VI summarizes the paper.

II. SYSTEM DESCRIPTION AND PROBLEM FORMULATION

Consider a class of nonlinear systems in canonical form,

$$
\begin{aligned}
\dot{x} &= Ax + Bf(x, u) \\
y &= Cx + \nu(t)
\end{aligned}
\tag{1}
$$

where $x \in \mathbb{R}^n$ represents the system state vector, and $u \in \mathbb{R}$ and $y \in \mathbb{R}$ denote the system input and output, respectively. The matrices A, B, and C are defined as

$$
A = \begin{bmatrix} 0 & 1 & 0 & \cdots & 0 \\ \vdots & \ddots & \ddots & \ddots & \vdots \\ 0 & \cdots & \ddots & \ddots & 1 \\ 0 & \cdots & \cdots & 0 & 0 \end{bmatrix}, B = \begin{bmatrix} 0 \\ \vdots \\ 0 \\ 1 \end{bmatrix}, C = \begin{bmatrix} 1 \\ 0 \\ \vdots \\ 0 \end{bmatrix}^T
$$

Furthermore, $\nu(t)$ expresses the output measurement noise with an unknown upper bound of $\bar{\nu}$, i.e., $\|\nu(t)\| \leq \bar{\nu}$, and $f(x, u)$ is an unknown nonlinear function. To guarantee the uniqueness of the system solution, $f(x, u)$ is assumed to be locally Lipschitz in its arguments over the domain of interest and zero in a compact positively invariant set Σ [7].

It is assumed that if all the system states are measurable, the following state feedback controller is capable of making the closed-loop system uniformly asymptotically stable concerning set Σ [7],

$$
\begin{aligned}
u &= g(x, \theta) \\
\dot{\theta} &= h(x, \theta)
\end{aligned}
\tag{2}
$$

where $g(\cdot)$ and $h(\cdot)$ are locally Lipschitz in their arguments over the domain of interest and globally bounded functions of x. Furthermore, let us denote an open connected subset of the corresponding region of attraction by $\mathcal{S}$. Note that the considered class of control signal (2) covers a wide range of control inputs. Such a control input can be designed using feedback linearizion approach, sliding mode scheme, adaptive techniques (conventional or intelligent), etc. Thus, the analysis provided in the subsequent sections are valid regardless of the

way that the controller has been designed. In other words, one can design a suitable state feedback controller separately and then replace the system states by the MHGO-based state estimations.

The understudy control problem is more general than the stabilization of an equilibrium point. In other words, lots of control problems (e.g., regulation, tracking, etc.) can be treated by properly defining the set Σ. For instance, the stabilization problem of the origin is a special case of the problem above in which $\Sigma = \{0\}$.

Since the assumption of availability of all system states is not always feasible in practice, the aforementioned controller cannot be applied to all real-life processes. To relax this assumption, it is required to estimate the system states suitably and feed them back to the controller. However, in this case, the stability of the closed-loop system should be investigated carefully. In the subsequent sections, the assumption of availability of all system states is removed by utilizing an observer-based controller, and the robustness of the closed-loop system when the system output is contaminated by measurement noise is analyzed.

III. OBSERVATION STRUCTURE

This section presents the structures of conventional HGO and MHGO. In addition, a brief comparison between these two state estimation strategies are provided to elucidate more on the advantages obtained from combining observations collected from different sources/observers.

A. High-gain Observer

The dynamical equation of a single HGO is as follows:

$$\dot{\hat{x}} = A\hat{x} + Bf_o(\hat{x}, u) + H(y - C\hat{x}) \tag{3}$$

where $H = \begin{bmatrix} \kappa_1/\epsilon & \kappa_2/\epsilon^2 & \cdots & \kappa_n/\epsilon^n \end{bmatrix}^T$ and $\epsilon \in (0, 1]$. The function $f_o(x, u)$ is a nominal model of $f(x, u)$ which is locally Lipschitz in its arguments, globally bounded in $\hat{x}$, and zero in Σ. In addition, κ_i are chosen such that the real parts of all roots of polynomial $P(s) = s^n + \kappa_1 s^{n-1} + \cdots + \kappa_{n-1}s + \kappa_n$ lie in the open left-half plane. Such a selection ensures that $A - HC$ is a Hurwitz matrix.

It is well-known that the single HGO (3) can estimate system state vector accurately by selecting sufficiently large gains. However, the classic HGO (3) suffers from two major issues:

(i) undesirable peaks exist in the transient response of the estimated states, and if they are fed into the controller, they may push the system into instability

(ii) when the measurement is noisy, one cannot choose the gain in observer (3) arbitrarily large. More clearly, selecting a large gain may yield a large steady state error.

In the following subsection, several HGOs with suitable initial conditions are run, and the collected state estimations are employed to estimate the system state vector in a manner such that the aforementioned issues are mitigated.

B. Multiple High-gain Observers

In this section, the MHGO structure and its capabilities in providing reliable state estimations are presented. Since this structure utilizes some properties of convex sets, it is useful to present the following lemma.

Lemma 1: [31] Let $\mathcal{K}$ be a convex subset of a linear space. Then, any element of the convex hull $\mathcal{K}$ of $\{q_1, \cdots, q_N\}$, i.e., $q \in \mathcal{K}$, can be expressed as $q = \sum_{i=1}^{N} \beta_i q_i$ where $\beta_i \in [0, 1]$ are constant terms and $\sum_{i=1}^{N} \beta_i = 1$.

In order to provide state estimations using multiple HGOs, inspired by [25], the dynamical equation for MHGO strategy is considered as follows:

$$\dot{\hat{x}}_i(t) = A\hat{x}_i(t) + H(y(t) - C\hat{x}_i(t))$$
$$\hat{x}_o(t) = \sum_{i=1}^{N} \hat{\beta}_i(t)\hat{x}_i(t) \tag{4}$$

where $i = 1, \cdots, N$, $\hat{x}_i$ is the state estimation obtained from the ith observer. Besides, $\hat{\beta}_i$ represent estimations of constant parameters β_i, and they are calculated such that the equality $\sum_{i=1}^{N} \hat{\beta}_i(t) = 1$ holds. Note that to be able to use Lemma 1, the number of observers should be larger than the number of state variables, i.e., $N \geq n+1$. Moreover, one can see that in contrast to multiple models/observers with switching, the MHGO does not need a large number of models and simultaneously utilize all available information. Regarding the parameters β_i, the following lemma is considered.

Lemma 2: Consider the state estimation (4). Let the initial conditions $\hat{x}_i(0)$ be chosen such that $x(0)$ lies in their convex hull. Then, there exist some positive constant terms $\bar{f}_0, \bar{\nu}, \beta_i$ with $\sum_{i=1}^{N} \beta_i = 1$ such that the state estimation error $e(t) = x(t) - \sum_{i=1}^{N} \beta_i \hat{x}_i(t)$ depends on $\epsilon \bar{f}_0$ and $\bar{\nu}/\epsilon^{n-1}$.

Proof: In order to prove the preceding lemma, let us use the facts that β_i are constant terms and $\sum_{i=1}^{N} \beta_i = 1$, and derive the dynamical equation of error $e(t)$ as follows:

$$\dot{e} = \dot{x} - \sum_{i=1}^{N} \beta_i \dot{\hat{x}}_i = \sum_{i=1}^{N} \beta_i \left(\dot{x} - \dot{\hat{x}}_i \right)$$

By substituting (1) and (4) into the preceding equation, one can get

$$\dot{e} = (A - HC)e + Bf(x, u) - H\nu(t) \tag{5}$$

Now, let us define a scaled version of the estimation error as $\eta = D(\epsilon)e$, where the matrix $D(\epsilon)$ is defined as follows:

$$D(\epsilon) = \begin{bmatrix} 1 & 0 & \cdots & 0 \\ 0 & \epsilon & \ddots & \vdots \\ \vdots & \ddots & \ddots & 0 \\ 0 & \cdots & 0 & \epsilon^{n-1} \end{bmatrix} \tag{6}$$

Taking the time derivative of the scaled error η and using (5), one can get

$$\dot{\eta} = \frac{1}{\epsilon}A_o\eta + \frac{1}{\epsilon}H_o\nu(t) + \epsilon^{n-1}Bf(x, u) \tag{7}$$

where $H_o = -\epsilon DH = \begin{bmatrix} -\kappa_1 & -\kappa_2 & \cdots & -\kappa_n \end{bmatrix}^T$ and

$$A_o = \epsilon D (A - HC) D^{-1} = \begin{bmatrix} -\kappa_1 & 1 & 0 & \cdots & 0 \\ -\kappa_2 & 0 & \ddots & \ddots & \vdots \\ \vdots & \vdots & \ddots & \ddots & 1 \\ -\kappa_n & 0 & \cdots & 0 & 0 \end{bmatrix}$$

Consider the Lyapunov function candidate $V_0(\eta) = \eta^T P_0 \eta$ for system (7), where $P_0 = P_0^T$ is a positive definite matrix whose the largest and the smallest eigenvalues are denoted by $\lambda_{\max}$ and $\lambda_{\min}$, respectively. It is assumed that P_0 satisfies the Lyapunov's equation, i.e.,

$$A_o^T P_0 + P_0 A_o = -I \tag{8}$$

Taking the time derivative of $V_0(\eta)$ and utilizing (7) and (8), yield

$$\dot{V}_0(\eta) = -\frac{1}{\epsilon}\|\eta\|^2 + \frac{2}{\epsilon}\eta^T P_0 H_o \nu(t) + 2\epsilon^{n-1}\eta^T P_0 B f(x,u) \tag{9}$$

Due to the boundedness of function $f(x,u)$ in the domain of interest, one has $\|f(x,u)\| \le \bar{f}_0$. Using this fact and performing some basic mathematical manipulations on (9), one can get

$$\dot{V}_0(\eta) \le -\frac{1}{2\epsilon}\|\eta\|^2 - \frac{\|\eta\|}{2\epsilon}\left(\|\eta\| - 4\epsilon^n \|P_0\|\bar{f}_0 - 4\|P_0 H_o\|\bar{\nu}\right)$$

This equation implies that $\dot{V}_0(\eta) \le -\frac{1}{2\epsilon}\|\eta\|^2$ as long as $\|\eta\| \ge 4\epsilon^n \|P_0\|\bar{f}_0 + 4\|P_0 H_o\|\bar{\nu}$. As a result, the set

$$\mathcal{S}_0 = \{\eta \in \mathbb{R}^n|\ V_0(\eta) \le \left(4\epsilon^n \|P_0\|\bar{f}_0 + 4\|P_0 H_o\|\bar{\nu}\right)^2 \lambda_{\max}\}$$

is an invariant set for the system.

Using the fact that the initial conditions of observers, $\hat{x}_i(0)$, are selected such that $x(0)$ lies in their convex hull, there exist constant terms β_i such that $x(0) = \sum_{i=1}^N \beta_i \hat{x}_i(0)$ or equivalently $e(0) = 0$ (see Lemma 1), and in turn, $\eta(0) = 0$. Therefore, the estimation error is initiated from inside of the invariant set $\mathcal{S}_0$; furthermore, we have $\lambda_{\min}\|\eta\|^2 \le V_0(\eta) \le \lambda_{\max}\|\eta\|^2$. According to these facts, it is valid to say that $\|\eta\| \le \sqrt{\frac{\lambda_{\max}}{\lambda_{\min}}}\left(4\epsilon^n \|P_0\|\bar{f}_0 + 4\|P_0 H_o\|\bar{\nu}\right)$. By using the preceding inequality and $\|e\| = \|D^{-1}\eta\| \le \frac{1}{\epsilon^{n-1}}\|\eta\|$, one can show that

$$\|e\| \le \sqrt{\frac{\lambda_{\max}}{\lambda_{\min}}}\frac{4\epsilon^n \|P_0\|\bar{f}_0 + 4\|P_0 H_o\|\bar{\nu}}{\epsilon^{n-1}} \tag{10}$$

Consequently, there exists a bounded term $\delta(t, \epsilon\bar{f}_0, \bar{\nu}/\epsilon^{n-1})$ such that $e(t) = \delta(t, \epsilon\bar{f}_0, \bar{\nu}/\epsilon^{n-1})$. It is worth mentioning that when there is no measurement noise, $\bar{\nu} = 0$, the upper bound on the norm of observation error becomes $\sqrt{\frac{\lambda_{\max}}{\lambda_{\min}}}4\epsilon\|P_0\|\bar{f}_0$. Therefore, in this case, the ultimate estimation error bound tends to zero as ϵ goes to zero. ∎

It is well-known that the stability and performance of observer-based control strategies greatly depend on the convergence rate of the observer. More clearly, as will be shown later, if the state estimation error enters an invariant set fast enough, the closed loop system is stable. As it was shown in Lemma 2, we have $e(t) = x(t) - \sum_{i=1}^N \beta_i \hat{x}_i(t) = \delta(t, \epsilon\bar{f}_0, \bar{\nu}/\epsilon^{n-1})$; hence the following equality holds.

$$x(t) = \sum_{i=1}^N \beta_i \hat{x}_i(t) + \delta(t, \epsilon\bar{f}_0, \bar{\nu}/\epsilon^{n-1}) \tag{11}$$

Now, let us define $e_o = x - \hat{x}_o$ and substitute (11) and (4) into it. Thus, we get

$$e_o(t) = \sum_{i=1}^N \beta_i \hat{x}_i - \sum_{i=1}^N \hat{\beta}_i \hat{x}_i + \delta(t, \epsilon\bar{f}_0, \bar{\nu}/\epsilon^{n-1})$$

By adding $x = \sum_{i=1}^N \hat{\beta}_i x$ to and subtracting $x = \sum_{i=1}^N \beta_i x$ from the right-hand side of the preceding equality ($\sum_{i=1}^N \hat{\beta}_i = \sum_{i=1}^N \beta_i = 1$), it is valid to conclude that

$$e_o(t) = \sum_{i=1}^N \tilde{\beta}_i e_i + \delta(t, \epsilon\bar{f}_0, \bar{\nu}/\epsilon^{n-1}) \tag{12}$$

where $\tilde{\beta} = \hat{\beta}_i - \beta_i$ and $e_i = x - \hat{x}_i$. It is clear that since the final estimation error $e_o(t)$ is the multiplication of two estimation errors $\tilde{\beta}_i$ and e_i, this observation error is capable of entering the invariant set very fast. In other words, this type of problem re-parameterization (converting the state estimation problem into estimation of constant parameters β_i) expedites the convergence process. To obtain estimations of β_i, the following RLS algorithm is employed,

$$\dot{\hat{\beta}} = -PE^T C^T(\tilde{y}_N + CE\hat{\beta}), \quad \hat{\beta}(0) = \hat{\beta}_0$$
$$\dot{P} = -PE^T C^T CEP, \qquad\qquad P(0) = \gamma I \tag{13}$$

where $\hat{\beta} = \begin{bmatrix} \hat{\beta}_1 & \hat{\beta}_2 & \cdots & \hat{\beta}_{N-1} \end{bmatrix}^T$, $\hat{\beta}_N = 1 - \sum_{i=1}^{N-1} \hat{\beta}_i$, $\tilde{y}_N = y - C\hat{x}_N$, $I \in \mathbb{R}^{(N-1)\times(N-1)}$ is the identity matrix, and γ is a positive constant. Furthermore, the ith column of $E(t)$ is defined as $\hat{x}_N(t) - \hat{x}_i(t)$.

Remark 1: It was shown that the convergence speed of the proposed observation scheme (4) and (13) depends on the convergence rate of both $\hat{x}_i$ and $\hat{\beta}_i$ (see (12)). On the other hand, it is well-known that the convergence rates of individual observers (4), $\hat{x}_i$, and the RLS algorithm (13), $\hat{\beta}_i$, depend on ϵ and γ, respectively. Thus, the need for considering a very small ϵ in conventional HGOs can be relaxed. To get the desired state estimation performance, the parameter ϵ needs to be selected large for making the ultimate estimation error $\delta(\cdot)$ small as well as avoiding the peaking, and the parameter γ should appropriately be chosen for improving the transient response and expediting the convergence process. In regard to the initial conditions $\hat{\beta}_i(0)$, if there is no a priori knowledge about how close the initial condition of the ith observer ($\hat{x}_i(0)$) is to the system states, one can set the initial weights equally, i.e., $\hat{\beta}_i(0) = \frac{1}{N}$. In the case that a prior knowledge exists, then we will give a higher initial weight to the closest observer.

IV. ROBUSTNESS ANALYSIS OF MHGO IN FEEDBACK CONTROL

It is well-known that performance of observer-based controllers are dictated by the utilized state estimation. Due to the advantages mentioned for the state estimation obtained from MHGO, such a estimation is used for control purposes in this section, and the robustness and stability analyses of the closed-loop system are fully discussed. In this case, one can feed the estimated system states $\hat{x}_o$ into the control signal (2), and get the output feedback controller as

$$u = g(\hat{x}_o, \theta)$$
$$\dot{\theta} = h(\hat{x}_o, \theta) \tag{14}$$

In the sequel, it will be shown that the MHGO-based control signal (14) is capable of recovering the performance of the state feedback controller.

To analyze the performance of the closed-loop system, first let us subtract (1) from (4) and get the error dynamics of each observer as follows:

$$\dot{e}_i(t) = (A - HC)e_i(t) + Bf(x, u) - H\nu(t) \qquad (15)$$

Now, define a scaled version of the estimation error $\eta_i = D(\epsilon)(x - \hat{x}_i)$, where $D(\epsilon)$ is as presented in (6). Taking the time derivative of the scaled error η_i and utilizing (15), result in

$$\epsilon\dot{\eta}_i(t) = A_o\eta_i(t) + \epsilon^n Bf(x, u) + H_o\nu(t) \qquad (16)$$

By using the fact that $\hat{\beta}_N = 1 - \sum_{i=1}^{N-1} \hat{\beta}_i$ and the definition of $\hat{x}_o$ (4), one can write the scaled state estimation error $\eta_o = D(\epsilon)(x - \hat{x}_o)$ as follows:

$$\eta_o = D(\epsilon)\left(\sum_{i=1}^{N-1} \hat{\beta}_i(x - \hat{x}_i) + \left(1 - \sum_{i=1}^{N-1} \hat{\beta}_i\right)(x - \hat{x}_N)\right)$$
$$= E_o\hat{\bar{\beta}} + \eta_N \qquad (17)$$

where the ith column of E_o is $\eta_i - \eta_N$. Besides, by employing (16), it is straightforward to show that

$$\epsilon\dot{E}_o = A_o E_o \qquad (18)$$

To get the dynamical equation of η_o, it is required to take the time derivative of (17), and employ (13), (16), (18). Thus, one can get

$$\dot{\eta}_o = \frac{1}{\epsilon}A_o\eta_o - E_o PE^T C^T C\left(e_N + E\hat{\bar{\beta}}\right)$$
$$- E_o PE^T C^T \nu(t) + \epsilon^{n-1}Bf(x, u) + \frac{1}{\epsilon}H_o\nu(t)$$

By employing the facts that $D^{-1}\eta_o = e_o = e_N + E\hat{\bar{\beta}}$, $CD^{-1} = C$, and $E = D^{-1}E_o$, one can rewrite the preceding equation as follows:

$$\dot{\eta}_o = \frac{1}{\epsilon}A_o\eta_o - E_o PE_o^T C^T C\eta_o$$
$$+ \left(-E_o PE_o^T C^T + \frac{1}{\epsilon}H_o\right)\nu(t) + \epsilon^{n-1}Bf(x, u) \qquad (19)$$

Now, let us employ (1) and (19) and write the system dynamics under the output feedback controller (14) as follows:

$$\dot{x} = Ax + Bf\left(x, g(x - D^{-1}\eta_o, \theta)\right) \qquad (20)$$
$$\epsilon\dot{\eta}_o = A_o\eta_o - \epsilon E_o PE_o^T C^T C\eta_o \qquad (21)$$
$$+ \left(-\epsilon E_o PE_o^T C^T + H_o\right)\nu(t) + \epsilon^n Bf\left(x, g(x - D^{-1}\eta_o, \theta)\right)$$

The obtained dynamical equations represent a system in the standard singularity perturbed form. In order to analyze the closed-loop system behavior, one needs to consider the following facts and lemma.

Fact 1: Because $P(t)$ is a positive definite matrix and $\dot{P}(t) \leq 0$ (see (13)), it is valid to conclude that $P(t)$ is bounded.

Fact 2: Since the matrix A_o is Hurwitz, the dynamical equation (18) results in a bounded term $E_o(t)$. In other words, there exist positive constants l_1 and λ such that $\|E_o(t)\| = \|\exp(\frac{1}{\epsilon}A_o t)E_o(0)\| \leq l_1 \exp(-\frac{1}{\epsilon}\lambda t)$.

Lemma 3: Consider the nonlinear function $h(\epsilon, \bar{\nu}) = \frac{4\epsilon^n \bar{f} + 2(a_1\epsilon + a_2)\bar{\nu}}{\epsilon^{n-1}}$ with positive constants $\bar{f}$, a_1, and a_2. Then,

there exist $\epsilon^* \in (0, 1]$, $\epsilon_1^* < \epsilon^*$ and $\epsilon_2^* > \epsilon^*$ such that for every $\bar{\nu} \in [0, \bar{\nu}^*(\epsilon^*)]$ and a given constant term $\bar{h}$, the inequality $h(\epsilon, \bar{\nu}) \leq \bar{h}$ holds for every $\epsilon \in [\epsilon_1^*, \epsilon_2^*]$.

Proof: To prove the lemma, we will first show that $h(\epsilon, \bar{\nu})$ has only one minimum point at ϵ^*. Then, this fact will be utilized to prove the lemma.

To prove the first part, it will be first shown that $\frac{\partial h}{\partial \epsilon} = 0$ has at most two roots. Then, all possible scenarios will be discussed, and it will be concluded that $h(\epsilon)$ has exactly one minimum point. In this regard, the partial derivative of $h(\epsilon)$ with respect to ϵ can be taken as follows:

$$\frac{\partial h}{\partial \epsilon} = \frac{4\bar{f}\epsilon^n - 2(n-2)a_1\bar{\nu}\epsilon - 2(n-1)a_2\bar{\nu}}{\epsilon^n} \qquad (22)$$

To find extrema of $h(\epsilon)$, we set $\frac{\partial h}{\partial \epsilon} = 0$. This is equivalent to $h_1(\epsilon) = 4\bar{f}\epsilon^n - 2(n-2)a_1\bar{\nu}\epsilon - 2(n-1)a_2\bar{\nu} = 0$ since $\epsilon \neq 0$. In order to show that the number of roots of $h_1(\epsilon) = 0$ is at most two, $\frac{\partial h_1}{\partial \epsilon}$ will be checked. By performing some basic manipulations, one can get $\frac{\partial h_1}{\partial \epsilon} = 4n\bar{f}\epsilon^{n-1} - 2(n-2)a_1\bar{\nu} = 0$, which has only one solution at $\epsilon = \left(\frac{2(n-2)a_1\bar{\nu}}{4n\bar{f}}\right)^{\frac{1}{n-1}}$. Hence, the sign of $\frac{\partial h_1}{\partial \epsilon}$ changes one time (from a negative value to a positive value), and in turn, it is valid to conclude that $h_1(\epsilon) = \frac{\partial h}{\partial \epsilon} = 0$ has at most two solutions.

Now, let us consider the following three possible cases: (i) $\frac{\partial h}{\partial \epsilon} = 0$ has no solution (ii) $\frac{\partial h}{\partial \epsilon} = 0$ has one solution (iii) $\frac{\partial h}{\partial \epsilon} = 0$ has two distinct solutions. Let us check some properties of function $h(\epsilon)$ and show that case (i) results in a contradiction. Since function $h(\epsilon)$ has a negative slope for small values of ϵ (see (22)), $\lim_{\epsilon\to 0^+} \frac{\partial h}{\partial \epsilon} < 0$, this function is indeed decreasing at the beginning. On the other hand, we have $\lim_{\epsilon\to 0^+} h(\epsilon) = +\infty$ and $\lim_{\epsilon\to+\infty} h(\epsilon) = +\infty$. Thus, the slope of this function should change its sign at some points, which contradicts with the assumption of having no solution for $\frac{\partial h}{\partial \epsilon} = 0$, i.e., case (i). For case (ii), let us assume that ϵ_1 denotes the root of $\frac{\partial h}{\partial \epsilon} = 0$. Since $\lim_{\epsilon\to 0^+} \frac{\partial h}{\partial \epsilon} < 0$ and both $\lim_{\epsilon\to 0^+} h(\epsilon)$ and $\lim_{\epsilon\to+\infty} h(\epsilon)$ tend to $+\infty$, ϵ_1 is the minimum point of function $h(\epsilon)$. On the other hand, we have $\epsilon \in (0, 1]$; thus, in this case, the minimum occurs at $\epsilon^* = \min\{\epsilon_1, 1\}$. For case (iii), let us denote the two distinct roots of $\frac{\partial h}{\partial \epsilon} = 0$ by ϵ_2 and ϵ_3. Using a similar discussion presented for cases (i) and (ii), one can conclude that at least one of these distinct roots should be the minimum point of function $h(\epsilon)$, e.g., ϵ_2. For the other root, i.e., ϵ_3, since we assumed that $\frac{\partial h}{\partial \epsilon}\big|_{\epsilon=\epsilon_3} = 0$, this point can be a minimum or a maximum or an inflection point of function $h(\epsilon)$. Because no function can have two consecutive minimum points (without having any maximum point in the between of them), ϵ_3 cannot be a minimum point. It cannot be a maximum point either since this assumption contradicts with the fact that $\lim_{\epsilon\to+\infty} h(\epsilon) = +\infty$. On the other hand, ϵ_3 is not an inflection point of function $h(\epsilon)$ since $\frac{\partial^2 h}{\partial \epsilon^2} = \frac{2(n-2)(n-1)a_1\bar{\nu}\epsilon + 2(n-1)na_2\bar{\nu}}{\epsilon^{n+1}} \neq 0$ for all bounded values of ϵ. In other words, case (iii) does not occur.

So far, it was proven that the function $h(\epsilon)$ has exactly one minimum at ϵ^*. To find the largest possible (less conservative) upper bound of $\bar{\nu}$, for a given constant $\bar{h}$, we need to check $h(\epsilon^*, \bar{\nu}) \leq \bar{h}$. Toward this end, by performing some basic manipulations on $\frac{4\epsilon^{*n}\bar{f} + 2(a_1\epsilon^* + a_2)\bar{\nu}}{\epsilon^{*n-1}} \leq \bar{h}$, one can conclude

that the upper bound of noise, $\bar{\nu}$, should be less than or equal to $\bar{\nu}^* = \frac{\epsilon^{*n-1}\bar{h}-4\epsilon^{*n}\bar{f}}{2(a_1\epsilon^*+a_2)}$. On the other hand, it is clear that if $\bar{\nu} \in [0, \bar{\nu}^*]$, then the equation $h(\epsilon, \nu) = \bar{h}$ has two solutions at $\epsilon_1^* < \epsilon^*$ and $\epsilon_2^* > \epsilon^*$. Hence, the inequality $h(\epsilon, \nu) \le \bar{h}$ holds for every $\epsilon \in [\epsilon_1^*, \epsilon_2^*]$. ∎

The following theorem summarizes performance recovery of the singularly perturbed closed-loop system in the presence of measurement noise (refer to (20) and (21)).

Theorem 1: Let us consider the dynamical system (1) with the control input (2). If the system states are estimated using the observer (4) with the adaptive law (13), then for any compact set $\mathcal{S}_1 \subseteq \mathcal{S}$ (where $\mathcal{S}$ is an open connected subset of the region of attraction) and any compact set $\mathcal{S}_2 \subseteq \mathbb{R}^n$, there exist constants $\bar{\nu}^*$, ϵ_1^* and ϵ_2^* such that for every $\|\nu(t)\| \le \bar{\nu}^*$, $\epsilon \in [\epsilon_1^*, \epsilon_2^*]$, the solution $(x, \hat{x}_o)$, starting in $\mathcal{S}_1 \times \mathcal{S}_2$, is bounded for all t. Furthermore, the adaptive parameters $\hat{\bar{\beta}}(t)$ and the individual observers estimations $\hat{x}_i(t)$ are bounded as well.

Proof: The proof of theorem is divided into two steps. First, we will guarantee boundedness of the state estimation error $x - \hat{x}_o$ and the system state x. Then, this information will be used in the second step to prove that all other signals in the closed-loop system are bounded as well.

Step 1 (boundedness of $x - \hat{x}_o$ and x): To prove the first step, a positive invariant set will be derived for the system dynamics which will guarantee boundedness of $x - \hat{x}_o$ and x. This step is composed of two sub-steps:

- In sub-step 1, it is guaranteed that $x - \hat{x}_o \in \mathcal{L}_\infty$ assuming that $x \in \mathcal{S}_c$ ($\mathcal{S}_c$ will be defined later).
- In sub-step 2, we will ensure that when $x(t)$ starts from inside of the set $\mathcal{S}_1 \subseteq \mathcal{S}_c$, $\eta_o(t)$ will enter the set $\mathcal{S}_3$ ($\mathcal{S}_3$ will be defined later) before that $x(t)$ leaves $\mathcal{S}_c$; then it will be shown that $\mathcal{S}_c \times \mathcal{S}_3$ is a positive invariant set, and in turn, $x(t)$ and $\eta_o(t)$ will remain inside the set $\mathcal{S}_c \times \mathcal{S}_3$ thereafter.

Step 1.1: Let us consider the Lyapunov function candidate $V_1(\eta_o) = \eta_o^T P_0 \eta_o$ for system (21). Taking the time derivative of this function and substituting (21) and (8) into it, yield

$$\dot{V}_1(\eta_o) = -\frac{1}{\epsilon}\eta_o^T \eta_o - 2\eta_o^T P_0 E_o P E_o^T C^T C \eta_o$$
$$+ 2\eta_o^T P_0 \left(-E_o P E_o^T C^T + \frac{1}{\epsilon} H_o\right)\nu(t) \qquad (23)$$
$$+ 2\epsilon^{n-1}\eta_o^T P_0 B f(x, u)$$

Due to the globally boundedness of controller u in its arguments and locally Lipschitz property of $f(x, u)$, one has $\|f(x, u)\| \le \bar{f}_0$ over a domain of interest $\mathcal{S}_c \subseteq \mathcal{S}$ ($\mathcal{S}_c$ will be defined later). By using the preceding inequality and performing some basic mathematical manipulations on (23), one can get

$$\dot{V}_1(\eta_o) \le -\frac{1}{\epsilon}\|\eta_o\|^2 - 2\eta_o^T P_0 E_o P E_o^T C^T C \eta_o$$
$$+ \left(a_1 + \frac{1}{\epsilon}a_2\right)\|\eta_o\|\bar{\nu} + 2\epsilon^{n-1}\|\eta_o\|\bar{f}$$

where $2\|P_0 E_o P E_o^T C^T\| \le a_1$, $a_2 = 2\|P_0 H_o\|$, and $\bar{f} = \|P_0\|\bar{f}_0$. With regard to Facts 1 and 2, one can conclude that constant a_1 is a bounded term.

Now let us define the compact set

$$\mathcal{S}_3 = \{\eta_o \in \mathbb{R}^n | \; V_1(\eta_o) \le \left(2\left(\epsilon a_1 + a_2\right)\bar{\nu} + 4\epsilon^n \bar{f}\right)^2 \lambda_{\max}\} \qquad (24)$$

Outside of the above set, one has $\dot{V}_1(\eta_o) \le -\frac{1}{2\epsilon}\|\eta_o\|^2 - 2\eta_o^T P_0 E_o P E_o^T C^T C \eta_o$. By using Fact 2 and performing some basic manipulations on the preceding inequality, one can get

$$\dot{V}_1(\eta_o) \le -\frac{1}{2\epsilon}\|\eta_o\|^2 + l_2 \exp(-\frac{2}{\epsilon}\lambda t)\|\eta_o\|^2 \qquad (25)$$

where $2l_1^2\|P_0\|\|P\|\|C^T C\| \le l_2$. Note that by utilizing Facts 1 and 2, it is straightforward to conclude that the positive constant l_2 is bounded. By using inequality $\lambda_{\min}\|\eta_o\|^2 \le V_1(\eta_o) \le \lambda_{\max}\|\eta_o\|^2$ and (25), one has

$$\dot{V}_1(\eta_o) \le \left(-\frac{1}{2\epsilon\lambda_{\max}} + \frac{l_2}{\lambda_{\min}}\exp(-\frac{2}{\epsilon}\lambda t)\right)V_1(\eta_o) \qquad (26)$$

where $\lambda_{\max}$ and $\lambda_{\min}$ denote the largest and smallest eigenvalues of the matrix P_0. Taking integral over (26), results in

$$V_1(t) \le V_1(0) \exp\left(-\frac{t}{2\epsilon\lambda_{\max}}\right) \exp\left(\frac{l_2\epsilon}{2\lambda\lambda_{\min}}\left(1 - \exp(-\frac{2}{\epsilon}\lambda t)\right)\right)$$

Since there exists a positive constant l_3 such that $\exp\left(\frac{l_2\epsilon}{2\lambda\lambda_{\min}}\left(1 - \exp(-\frac{2}{\epsilon}\lambda t)\right)\right) \le l_3$, one can get

$$V_1(t) \le V_1(0)l_3 \exp\left(-\frac{t}{2\epsilon\lambda_{\max}}\right) \qquad (27)$$

Therefore, if η_o is outside of the compact set $\mathcal{S}_3$ (24), there exists a finite time $T(\epsilon)$ after which η_o will enter that set. To obtain a closed form for $T(\epsilon)$, the preceding inequality can be utilized to get

$$T(\epsilon) = 4\epsilon\lambda_{\max} \ln\left(\frac{\sqrt{V_1(0)l_3}}{4\epsilon^n \bar{f}\sqrt{\lambda_{\max}}}\right) \qquad (28)$$

On the other hand, as long as the scaled state estimation error is inside $\mathcal{S}_3$, $\|x - \hat{x}_o\| = \|D^{-1}\eta_o\| \le \frac{1}{\epsilon^{n-1}}\|\eta_o\|$ satisfies the following inequality

$$\|x - \hat{x}_o\| \le \sqrt{\frac{\lambda_{\max}}{\lambda_{\min}}}h(\epsilon, \bar{\nu}) \qquad (29)$$

where $h(\epsilon, \bar{\nu}) = \frac{4\epsilon^n \bar{f} + 2(a_1\epsilon + a_2)\bar{\nu}}{\epsilon^{n-1}}$. Hence, we showed that $\eta_o(t)$ is bounded; however, the provided analyses were based on the assumption that $x(t) \in \mathcal{S}_c$. In the sequel, the analysis of this part is divided into two phases. First, we will ensure that when $x(t)$ starts from inside of the set $\mathcal{S}_1 \subseteq \mathcal{S}_c$, $\eta_o(t)$ will enter the set $\mathcal{S}_3$ before that $x(t)$ leaves $\mathcal{S}_c$, i.e., the provided analysis for $\eta_o(t)$ is valid during this time interval. Second, it will be shown that $\mathcal{S}_c \times \mathcal{S}_3$ is a positive invariant set, and in turn, $x(t)$ and $\eta_o(t)$ will remain inside the set $\mathcal{S}_c \times \mathcal{S}_3$ thereafter.

Step 1.2: Since the system dynamics are in the form of standard singularly perturbed systems [7], let us substitute $\eta_o = 0$ into (20) and get

$$\dot{x} = Ax + Bf(x, g(x, \theta)) \qquad (30)$$

It is obvious that the reduced system is identical to the system under the state feedback controller (2), and in turn, uniformly asymptotically stable with respect to the positively invariant set

Σ. According Lyapunov's converse Theorem [7], there exists a Lyapanuv's function $V_2(x)$ and positive definite functions $U_1(x)$, $U_2(x)$, and $U_3(x)$ for system (30) such that

$$
\begin{aligned}
V_2(x) = 0 &\iff x \in \Sigma \\
U_1(x) &\le V_2(x) \le U_2(x) \\
\dot{V}_2(x) &\le -U_3(x) \\
\lim_{x \to \partial \mathcal{S}} U_1(x) &= \infty
\end{aligned}
\tag{31}
$$

where $\mathcal{S}$ is an open connected subset of the region of attraction; moreover there exists $c \ge \max_{x \in \mathcal{S}_1} V_2(x)$ such that $\mathcal{S}_1 \subseteq \mathcal{S}_c = \{x \in \mathbb{R}^n |\, V_2(x) \le c\} \subseteq \mathcal{S}$.

Since the nonlinear function $f(x,u)$ is locally Lipschitz function and $u = g(x - D^{-1}\eta_o)$ is globally bounded over the set of interest $\mathcal{S}_c$, one has

$$
\|\dot{x}\| = \|Ax + Bf(x, g(\cdot))\| \le a_5
$$

where $a_5 > 0$ is a constant term. Taking integral over both sides of the preceding equation and using the fact that $\|\int_0^t \dot{x} d\tau\| \le \int_0^t \|\dot{x}\| d\tau$, yields $\|x(t) - x(0)\| \le a_5 t$. Moreover, we have $x(0) \in \mathcal{S}_1 \subseteq \mathcal{S}_c$; thus the inequality $\|x(t)-x(0)\| \le a_5 t$ implies that there exists T_1 such that $x(t)$ is inside the set $\mathcal{S}_c$ as long as $t \le T_1$. On the other hand, since $T(\epsilon)$ tends to zero as $\epsilon \to 0$ (refer to (28)), there exists a constant term ϵ_3^* such that for $\epsilon \le \epsilon_3^*$ we have $T(\epsilon) \le T_1$. In other words, the scaled state estimation error $\eta_o(t)$ enters the set $\mathcal{S}_3$ fast enough before that the system states $x(t)$ leave the set $\mathcal{S}_c$.

In the next step, it will be shown that if (x, η_o) lies inside of the set $\mathcal{S}_c \times \mathcal{S}_3$, this pair will always remain there. In other words, $\mathcal{S}_c \times \mathcal{S}_3$ is a positive invariant set. In this regard, by using the Lyapunov's function $V_2(x)$ for closed-loop system (20), one can get

$$
\dot{V}_2(x) \le -U_3(x) + \frac{\partial V_2}{\partial x} B\left(f(x, D^{-1}\eta_o) - f(x)\right)
$$

Due to the fact that $\|\frac{\partial V_2}{\partial x}\| \le a_3$ and the Lipschitz property of function $f(\cdot)$ over the domain of interest, it is valid to conclude that $\dot{V}_2(x) \le -U_3(x) + a_3 a_4 \|D^{-1}\eta_o\|$ where $a_4 \ge 0$ denotes the Lipschitz constant. Inside of the set $\mathcal{S}_c \times \mathcal{S}_3$ the presented upper bound in (29) is valid; thus by utilizing this upper bound and $\|D^{-1}\eta_o\| = \|x - \hat{x}_o\|$, the preceding inequality can be rewritten as follows:

$$
\dot{V}_2(x) \le -U_3(x) + \sqrt{\frac{\lambda_{\max}}{\lambda_{\min}}} a_3 a_4 h(\epsilon, \bar{\nu})
$$

By setting $\bar{h} = \sqrt{\frac{\lambda_{\min}}{\lambda_{\max}}} \frac{1}{a_3 a_4} \min_{x \in \partial \mathcal{S}_c} U_3(x)$ in Lemma 3, we get $\dot{V}_2(x) \le 0$ for $\bar{\nu} \in [0, \bar{\nu}_1^*]$ and $\epsilon \in [\epsilon_4^*, \epsilon_5^*]$. On the other hand, ϵ_3^* (obtained earlier for ensuring $T(\epsilon) \le T_1$ for all $\epsilon \le \epsilon_3^*$) gives us an upper bound for the measurement noise, i.e., $\bar{\nu}_2^* = \frac{\epsilon_3^{*n-1}\bar{h} - 4\epsilon_3^{*n}\bar{f}}{2(a_1\epsilon_3^* + a_2)}$. Thus, the parameters $\bar{\nu}^*$, ϵ_1^*, and ϵ_2^* (used in the theorem) can be defined as $\bar{\nu}^* = \min\{\bar{\nu}_1^*, \bar{\nu}_2^*\}$, $\epsilon_1^* = \epsilon_4^*$, and $\epsilon_2^* = \min\{\epsilon_3^*, \epsilon_5^*\}$. Note that we showed that $\dot{V}_1(\eta_o) \le 0$ and $\dot{V}_2(x) \le 0$ for all $(x(t), \eta_o(t)) \in \mathcal{S}_c \times \mathcal{S}_3$. Hence, the set $\mathcal{S}_c \times \mathcal{S}_3$ is a positive invariant set.

In summary, we proved that if $x(0) \in \mathcal{S}_1 \subseteq \mathcal{S}_c$ and η_o is outside of the set $\mathcal{S}_3$, then $x(t)$ and $\eta_o(t)$ will enter the set $\mathcal{S}_c \times \mathcal{S}_3$ after $T(\epsilon)$ units of time and will remain there for $t > T(\epsilon)$. This means that the solution $(x(t), \hat{x}_o(t))$ is bounded.

Step 2 (boundedness of $\hat{x}_i$ and $\hat{\beta}_i$): To complete the proof and ensure boundedness of the other signals of the closed-loop system, it is needed to guarantee that $\hat{x}_i, \hat{\bar{\beta}} \in \mathcal{L}_\infty$. Toward this end, first let us show that each observer yields a bounded state estimation vector, i.e., $\hat{x}_i \in \mathcal{L}_\infty$. In this regard, one can rewrite dynamical equation (4) as

$$
\dot{\hat{x}}_i(t) = (A - HC)\hat{x}_i(t) + H\left(Cx(t) + \nu(t)\right)
\tag{32}
$$

It was proven earlier that $x(t)$ belongs to $\mathcal{L}_\infty$; moreover $\nu(t)$ is bounded as well. Therefore, equation (32) represents a linear system with Hurwitz matrix $A - HC$ and bounded input $Cx(t) + \nu(t)$, and in turn, $\hat{x}_i \in \mathcal{L}_\infty$.

To prove that $\hat{\bar{\beta}} \in \mathcal{L}_\infty$, let us take integrate over (13) and get $\hat{\bar{\beta}}(t) - \hat{\bar{\beta}}(0) = -\int_0^t PE^T C^T (\tilde{y}_N + CE\hat{\bar{\beta}})d\tau$, and in turn, one has $\|\hat{\bar{\beta}}(t)\| \le \|\hat{\bar{\beta}}(0)\| + \|\int_0^t PE^T C^T (\tilde{y}_N + CE\hat{\bar{\beta}})d\tau\|$. Since $C\left(\tilde{x}_N + E\hat{\bar{\beta}}\right) + \nu(t) = C\tilde{x}_o + \nu(t)$, the preceding inequality can be rewritten as

$$
\|\hat{\bar{\beta}}(t)\| \le \|\hat{\bar{\beta}}(0)\| + \int_0^t \|PE^T C^T (C\tilde{x}_o + \nu)\| d\tau
\tag{33}
$$

As it was shown earlier $\tilde{x}_o = D^{-1}\eta_o \in \mathcal{L}_\infty$; thus $C\tilde{x}_o + \nu$ belongs to $\mathcal{L}_\infty$. Using the preceding equality, Facts 1 and 2, and (33), one has $\|\hat{\bar{\beta}}(t)\| \le \|\hat{\bar{\beta}}(0)\| + a_6 \int_0^t \exp(-\frac{1}{\epsilon}\lambda\tau)d\tau$, with $l_1\|P\|\|C\tilde{x}_o + \nu\| \le a_6$ where a_6 is a bounded constant. Hence, one has $\|\hat{\bar{\beta}}(t)\| \le \|\hat{\bar{\beta}}(0)\| + \frac{a_6\epsilon}{\lambda}\left(1 - \exp(-\frac{\lambda}{\epsilon}t)\right)$, and it is valid to conclude that $\hat{\bar{\beta}} \in \mathcal{L}_\infty$. ∎

V. SIMULATION RESULTS

In this section, two simulation results are presented to shed some light on the presented theoretical discussions. In the first simulation, a numerical example is considered and the obtained results for MHGO-based controller are compared with the conventional HGO-based approach as well as HGO with switching gain strategy [17]. In the second example, simulations are carried out on a mechanical system, and the superiority of the MHGO-based approach over conventional HGO-based schemes and multi-observer-based approaches is shown.

A. Example 1: Underwater Vehicle

In this subsection, a simplified model of underwater vehicle in yaw with dynamical equation of

$$
\ddot{\psi} + a\dot{\psi}|\dot{\psi}| = u
$$

is selected for simulation purposes, where ψ denotes the heading angle and a is a positive constant. Let us assume that only the heading angle is measured and that measurement is contaminated by noise $\nu(t)$, i.e., $y = \psi + \nu(t)$. In this simulation, $a = 1$ and the measurement noise, generated by Matlab uniform random number block with sampling time 0.0001, is in the interval $[-0.01, 0.01]$.

The control objective is to steer the heading angle to follow the sinusoidal wave $y_d = 5 + \sin(2t)$. It is obvious that the state feedback controller $u = a\dot{\psi}|\dot{\psi}| + \ddot{y}_d + 4(\dot{\psi} - \dot{y}_d) + 4(\psi - y_d)$
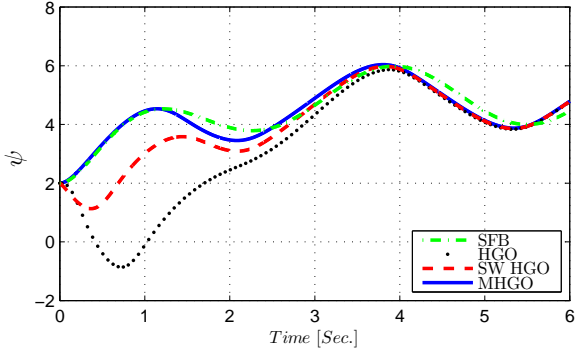
Fig. 1: Evolution of $\psi(t)$ using state feedback, HGO-based, Switching HGO-based, and MHGO-based controllers.
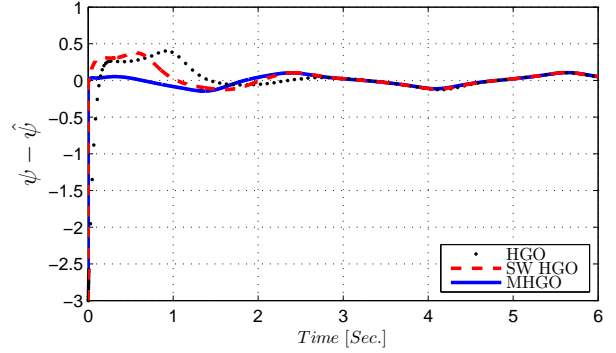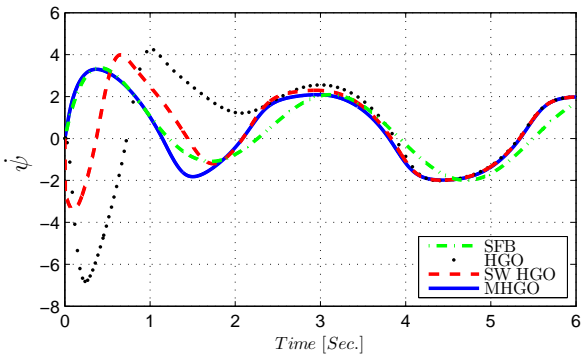

Fig. 2: Evolution of $\dot{\psi}(t)$ using state feedback, HGO-based, Switching HGO-based, and MHGO-based controllers.

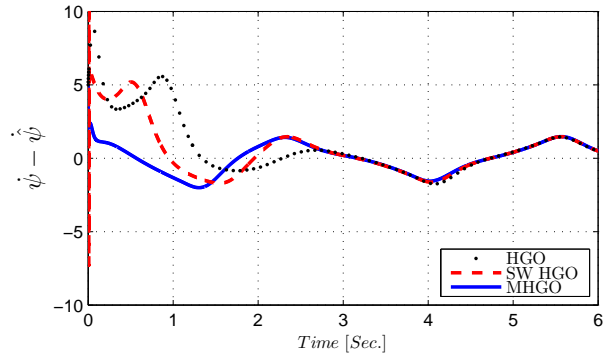Fig. 3: State estimation errors of ψ using conventional HGO, Switching HGO and MHGO.

Fig. 4: State estimation errors of $\dot{\psi}$ using conventional HGO, Switching HGO and MHGO.

can force the heading angle to track y_d asymptotically. Since $\dot{\psi}$ is not measurable, it should be reconstructed appropriately and fed into the above controller. As stated in the previous section, MHGOs are capable of providing such an estimation; hence they are used in this regard. For comparison purposes, simulations are also performed by utilizing the conventional HGO and the HGO with switching gain [17]. The basic idea behind the latter observation scheme, HGO with switching gain, is to switch from a small gain to a larger gain. More clearly, a small value for ϵ is employed in the beginning to get a fast response, then it is switched to a larger value to avoid large steady observation errors caused by the measurement noise [17].

The design parameters of the conventional HGO are selected as $\epsilon = 0.15$, $\kappa_1 = 2$, $\kappa_2 = 1$. Furthermore, the design parameters of the switching HGO change from $\epsilon = 10^{-3}$, $\kappa_1 = 71$, $\kappa_2 = 70$ to $\epsilon = 0.15$, $\kappa_1 = 2$, $\kappa_2 = 1$. Besides, it is assumed that the implemented control effort by the actuator is restricted by amplitude of 500. For the MHGO, to be able to run the adaptive laws (13), initial conditions of the RLS algorithm are selected as follows: $\gamma = 10^3$, $\hat{\beta}_1(0) = \hat{\beta}_2(0) = 0$, and in turn $\hat{\beta}_3(0) = 1 - \sum_{i=1}^{2} \hat{\beta}_i(0) = 1$. In addition, parameters κ_i and ϵ are set equal to the corresponding parameters of the conventional HGO. It is clear that the three approaches will eventually have $\epsilon = 0.15$, and in turn, all of them will affect the measurement noise with the same ϵ, which allows us to make

an accurate comparison. Moreover, the initial conditions of the multiple observers, employed in MHGO, are required to be selected such that the initial system states, i.e., $x(0) = \begin{bmatrix} 0 & 0 \end{bmatrix}^T$ lie in their convex hull. Toward this end, three observers are initiated from $\hat{x}_1(0) = \begin{bmatrix} +5 & +5 \end{bmatrix}^T$, $\hat{x}_2(0) = \begin{bmatrix} -5 & +5 \end{bmatrix}^T$, and $\hat{x}_3(0) = \begin{bmatrix} +5 & -5 \end{bmatrix}^T$; thus $\hat{x}_o$ starts from $\sum_{i=1}^{3} \hat{\beta}_i(0)\hat{x}_i(0) = \begin{bmatrix} +5 & -5 \end{bmatrix}^T$. To make the simulation results more comparable, the initial condition of the conventional HGO and HGO with switching are set equal to $\hat{x}_o(0) = \begin{bmatrix} +5 & -5 \end{bmatrix}^T$ as well.

The evolution of system states are depicted in Figs. 1 and 2. From these two figures, it is clear that the MHGO-based controller recovers performance of the state feedback controller faster than the two others. Also, due to the existence of the measurement noise on the system output $y(t)$, the controllers based on these observation strategies result in a bounded error. The state estimation process is also presented in Figs. 3 and 4. The obtained observation results are also in commensurate with the provided discussions. These figures show that because a small value is considered for ϵ in the transient phase in switching gain approach, this scheme reconstructs system states faster than the conventional HGO. Nonetheless, as it is well-known in the control literature, such a selection yields a large overshoot in the beginning of the estimation (see Fig. 5), which is not preferable in practice. The MHGO, on the other hand, provides satisfactory performance in terms of the convergence rate and peaking avoidance. Because, during
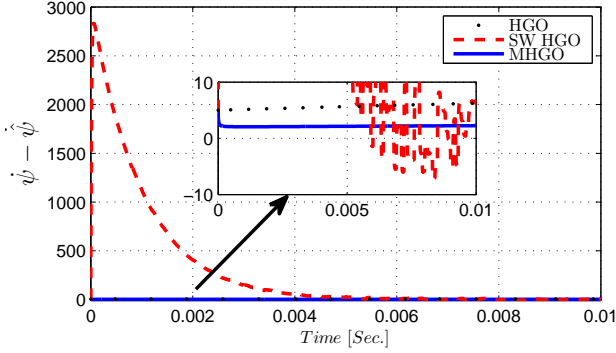
Fig. 5: State estimation errors of $\dot{\psi}$ during the transient phase using conventional HGO, Switching HGO and MHGO.

Fig. 6: A schematic of the system considered in example 2 [32].

the transient phase, the adaptive terms $\hat{\beta}_i$, presented for re-parameterizing the observation problem and combining the estimations of each observer, assist the observation structure to result in better estimations (see Remark 1). Note that in the long run $\hat{\beta}_i$ converge to their final values and since $\sum_{i=1}^{3} \hat{\beta}_i = 1$, MHGO behaves similarly to a single HGO.

B. Example 2: Connected Inverted Pendulums on Carts

Consider two inverted pendulums mounted on two carts and connected by a spring, as shown in Fig. 6. The governing dynamical equation of this mechanical system can be expressed as [32],

$$
\begin{aligned}
\dot{x}_{11} &= x_{12} \\
\dot{x}_{12} &= \mathcal{F}_{11}(x) + \mathcal{F}_{12} u_1 \\
\dot{x}_{21} &= x_{22} \\
\dot{x}_{22} &= \mathcal{F}_{21}(x) + \mathcal{F}_{22} u_2 \\
y &= \begin{bmatrix} x_{11} & x_{21} \end{bmatrix}^T + \nu(t)
\end{aligned}
\tag{34}
$$

where x_{k1} and x_{k2} $(k = 1, 2)$ represent the vertical angle of the kth pendulum θ_k and its angular velocity $\dot{\theta}_k$, respectively, $x = \begin{bmatrix} x_{11} & x_{12} & x_{21} & x_{22} \end{bmatrix}^T$ is the system state vector, $\nu(t) = \begin{bmatrix} \nu_1(t) & \nu_2(t) \end{bmatrix}^T$ denotes measurement noise, $\mathcal{F}_{k1}(x) = \left(\frac{g}{cl} - ka \frac{a-cl}{cml^2} \right) x_{k1} - \frac{m}{M} \sin(x_{k1}) x_{k2}^2 + ka \frac{a-cl}{cml^2} x_{j1}$ and $\mathcal{F}_{k2}(x) = \frac{1}{cml^2}$ with $k, j = 1, 2$ and $k \neq j$. In this simulation, the following values are considered for system parameters: mass of pendulum $m = 1$ kg, mass of cart $M = 5$ kg, constant term $c = \frac{m}{m+M}$, distance of the cart from the spring along with the bar $a = 0.2$ m, length of pendulum $l = 1$ m, spring constant $k = 1$ N/m, and gravity acceleration $g = 9.8$ m/s^2.

In order to make the closed-loop system asymptotically stable and force its output vector to track the desired trajectory $y_d = \begin{bmatrix} y_{1d} & y_{2d} \end{bmatrix}^T = \begin{bmatrix} 0.3\sin(t) & 0.3\cos(t) \end{bmatrix}^T$, the state feedback controller

$$
u_k = \frac{1}{\mathcal{F}_{k2}} \left(-\mathcal{F}_{k1} + \ddot{y}_{kd} - 7(x_{k2} - \dot{y}_{kd}) - 12(x_{k1} - y_{kd}) \right)
$$

which is saturated outside $\begin{bmatrix} -50 & +50 \end{bmatrix}$, is considered. In the sequel, the state reconstruction process is performed using three different approaches, namely a single HGO, multi-observe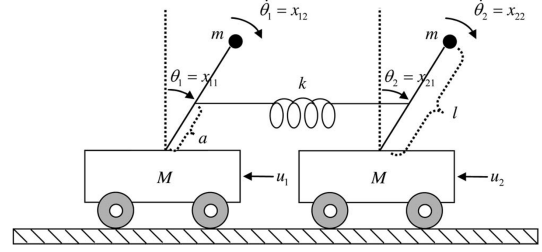r, and MHGO, and capabilities of these observation strategies in recovering performance of the state feedback controller are compared.

Note that (34) is a multi-input multi-output (MIMO) system, hence, it is required to explain how the MHGO scheme can be employed for estimating the system states. Toward this end, by using the fact that (34) represents a special class of MIMO systems with two subsystems in normal form, one can employ two sets of MHGO for state estimation of the overall system. One MHGO uses $y_1 = x_{11} + \nu_1(t)$ to estimate x_{11} and x_{12}, and the other one employs $y_2 = x_{21} + \nu_2(t)$ for estimating x_{21} and x_{22}. Each set of MHGO has N_k HGOs and the parameters estimations $(\hat{\beta}_{k1}, \hat{\beta}_{k2}, \cdots, \hat{\beta}_{kN_k})$ obtained from the RLS algorithm (13). It is clear that the aforementioned approach can be easily extended to a class of MIMO nonlinear systems consisted of more than two $(k > 2)$ subsystems in normal form.

To carry out the simulations, the initial conditions of the system are considered as $x(0) = \begin{bmatrix} 1 & 0 & 1 & 0 \end{bmatrix}^T$, and the measurement noise vector $\nu(t)$ is generated by two uniform random number blocks of Matlab Simulink with the values restricted to the interval $\begin{bmatrix} -0.02 & +0.02 \end{bmatrix}$ and sampling time 0.0001. Note that from this point forward, the superscript $k = 1, 2$ is used to denote the state estimation of subsystem k. In order to investigate the performance of conventional HGO-based controller, the state variables of each subsystem are estimated using a single HGO. For that, the design parameters and initial conditions of the kth observers are selected as: $\kappa_{k1} = 2$, $\kappa_{k2} = 1$, $\epsilon_k = 0.05$, $\hat{x}^k(0) = \begin{bmatrix} +3 & -3 \end{bmatrix}^T$. In multi-observer approach, N_k HGOs are run from various initial conditions to estimate states of the kth subsystem, and at each time instant, the performance criterion μ_{ki} obtained from $\dot{\mu}_{ki} = -\alpha \mu_{ki} + (y - \hat{y}_{ki})^2 :\ \mu_{ki}(0) = 0, \alpha = 0.1 > 0$ is checked to find the best observer [28]. More clearly, the best observer for subsystem k is chosen as $\sigma_k(t) = \underset{i}{\operatorname{argmin}} (\mu_{ki}(t))$, and in turn, the best estimation is $\hat{x}_{mul}^k = \hat{x}_{\sigma_k}$. For multi-observer approach, we will use three observers, $N_k = 3$, with initial conditions $\hat{x}_1^k(0) = \begin{bmatrix} +3 & +3 \end{bmatrix}^T$, $\hat{x}_2^k(0) = \begin{bmatrix} -3 & +3 \end{bmatrix}^T$, and $\hat{x}_3^k(0) = \begin{bmatrix} +3 & -3 \end{bmatrix}^T$ to estimate the states of subsystem k. Moreover, the rest of design parameters of the HGOs employed in the multi-observer method are chosen the same as the single HGO. To be able to make a reasonable comparison between the performance recovery of the MHGO-based controller and the aforementioned methods, the design parameters (i.e., κ_{k1}, κ_{k2}, ϵ_k), the number of observers (i.e., N_k), and initial conditions
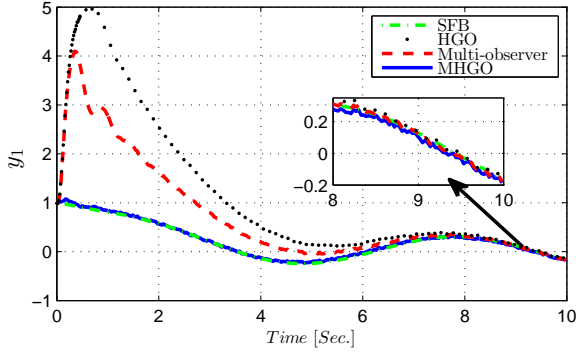
Fig. 7: Evolution of $y_1 = x_{11} + \nu_1(t)$ using state feedback, HGO-based, multi-observer-based, and MHGO-based controllers with $N_k = 3$.
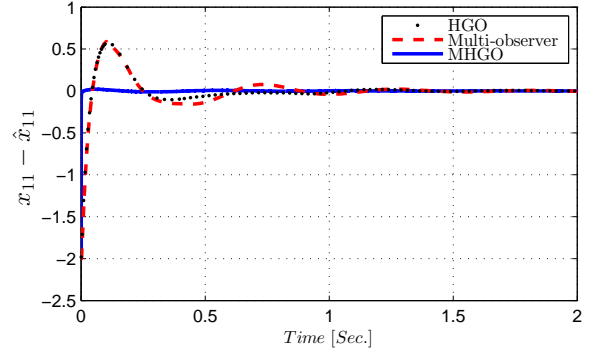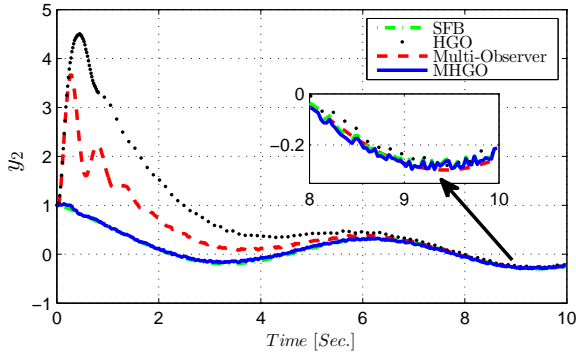

Fig. 8: Evolution of $y_2 = x_{21} + \nu_2(t)$ using state feedback, HGO-based, multi-observer-based, and MHGO-based controllers with $N_k = 3$.
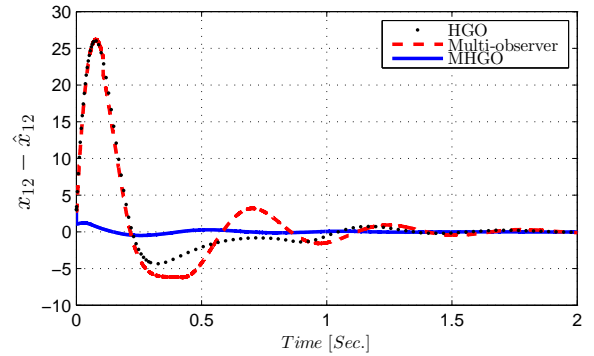

Fig. 9: Estimation error of first state, x_{11}, using conventional HGO, multi-observer, and MHGO with $N_k = 3$.

Fig. 10: Estimation error of second state, x_{12}, using conventional HGO, multi-observer, and MHGO with $N_k = 3$.

(i.e., $\hat{x}_i^k, i = 1, \cdots, N_k$) of MHGO are set equal to the ones selected for the multi-observer scheme. The RLS algorithm design parameters are considered as $P_k(0) = 10^3 I_{2\times 2}$, $\hat{\beta}_{k1} = \hat{\beta}_{k2} = 0, \hat{\beta}_{k3} = 1$. Thus, it is clear that such a selection results in $\hat{x}_o^k(0) = \sum_{i=1}^3 \hat{\beta}_{ki}(0)\hat{x}_i^k(0) = \hat{x}_3^k(0)$. Furthermore, $\sigma_k(0)$ in multi-observer is set as 3; hence all the observers have the same initial condition, i.e., $\hat{x}_o^k(0) = \hat{x}_{mul}^k(0) = \hat{x}^k(0)$.

The performance of the system states under the state feedback controller as well as the discussed output feedback controllers are illustrated in Figs. 7 and 8. These two figures obviously show that although the multi-observer-based controller yields a better response in comparison to the conventional HGO-based method, it does not outperform the MHGO-based controller. In other words, the MHGO-based controller has recovered the performance of the state feedback controller much faster than the other two methodologies. As discussed earlier and it is obvious from the zoomed parts in Figs. 7 and 8, performance of the state feedback controller cannot be recovered perfectly due to the existence of measurement noise $\nu(t)$. Because of the space limitation and the fact the two subsystems behave similarly, only the observation errors of the first subsystem are provided (Figs. 9 and 10). According to these figures, one can easily see that the state estimation errors of MHGO strategy converge to a small neighborhood

of the origin rapidly.

As mentioned in [28], [29], the multi-observer approach provides better results when the number of observers is increased. This implies that to assure that at least one of the models is sufficiently close to the plant, a quite large number of models is required. Hence, to make a more comprehensive comparison and show that the MHGO-based controller can outperform the multi-observer-based controller even when the number of observers are increased, another simulation with $N_k = 81$ is carried out. In this simulation, all the design parameters are chosen the same as the previous scenario. For providing the initial conditions of observers for subsystem k, four points $\begin{bmatrix} +3 & +3 \end{bmatrix}^T$, $\begin{bmatrix} +3 & -3 \end{bmatrix}^T$, $\begin{bmatrix} -3 & +3 \end{bmatrix}^T$, and $\begin{bmatrix} -3 & -3 \end{bmatrix}^T$ are considered as the vertices of uncertainty region $\mathcal{K}_k$, within which the initial conditions of subsystem k lies. Then, $\mathcal{K}_k$ is sampled uniformly to obtain 81 initial conditions for each set of observers. Simulation results are presented in Figs. 11-14. Figs. 11 and 12 clearly show that performance of the multi-observer-based approach is improved in comparison to the multi-observer with $N_k = 3$ (see Figs. 7 and 8); however, it is computationally more expensive than that case. These figures also demonstrate that the MHGO-based control approach results in a better performance in this scenario as well. It is worth noting that in these simulations the MHGO-based controller with $N_k = 3$ also outperforms the multi-observer-based controller with $N_k = 81$, which demonstrates
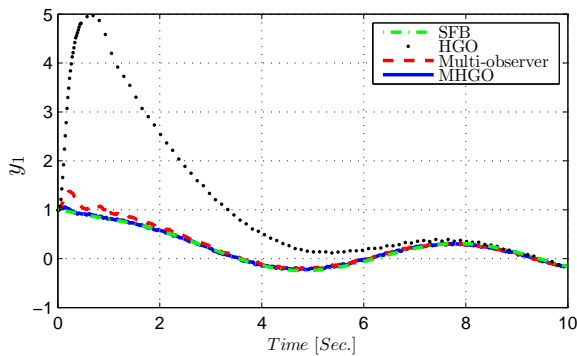
Fig. 11: Evolution of $y_1 = x_{11} + \nu_1(t)$ using state feedback, HGO-based, multi-observer-based, and MHGO-based controllers with $N_k = 81$.
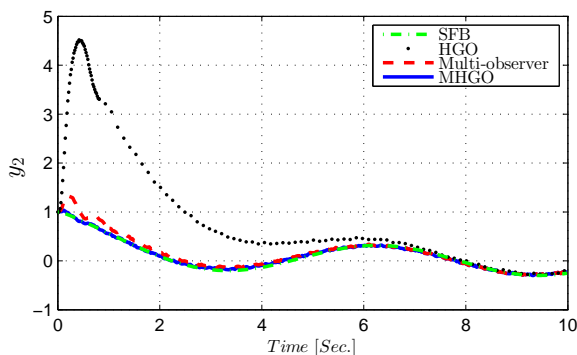

Fig. 12: Evolution of $y_2 = x_{21} + \nu_2(t)$ using state feedback, HGO-based, multi-observer-based, and MHGO-based controllers with $N_k = 81$.

the superiority of the MHGO-based strategy (refer to Figs. 7, 8, 11, 12). The obtained observations errors are also shown in Figs. 13 and 14, based on which it is clear that the MHGO scheme forces the observation errors to tend to a small neighborhood of the origin faster than other methods.

VI. CONCLUSIONS

This paper investigates the analysis of the performance of MHGO-based controllers when the system output is contaminated by measurement noise. It is well-known that in this case, increasing the gain of a single observer deteriorates the steady state bound of estimation error. Hence, one cannot choose an arbitrarily large gain to speed up the transient response, which is necessary for control purposes. The MHGO utilizes the observations obtained from various sources and introduces new design parameters. In turn, it provides a suitable tool for solving the aforementioned trade-off in conventional HGO. The necessary conditions under which such a structure was capable of recovering performance of the state feedback controllers in the presence of measurement noise were derived, and the stability of the closed-loop system was investigated. Two simulations were carried out for comparison purposes and to validate the theoretical discussions.

Several simulations performed on various dynamical systems have shown that the MHGO-based control strategy has a
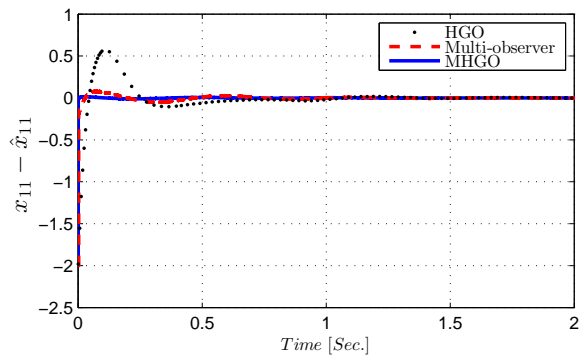

Fig. 13: Estimation error of first state, x_{11}, using conventional HGO, multi-observer, and MHGO with $N_k = 81$.
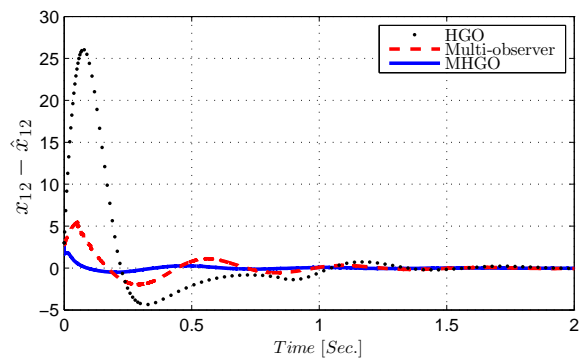

Fig. 14: Estimation error of second state, x_{21}, using conventional HGO, multi-observer, and MHGO with $N_k = 81$.

larger region of attraction in comparison to the conventional HGO. Further investigation of this property and providing a rigorous proof for that is worthwhile.

REFERENCES

[1] J. C. Doyle and G. Stein, "Robustness with observers," *IEEE Transactions on Automatic Control*, vol. 24, no. 4, pp. 607–611, 1979.
[2] R. E. Kalman, "A new approach to linear ltering and prediction problems," *Journal of Basic Engineering*, vol. 82, no. 1, pp. 35–45, 1960.
[3] B. Chen, G. Hu, D. W. C. Ho, W. Zhang, and L. Yu, "Distributed robust fusion estimation with application to state monitoring systems," *IEEE Transactions on Systems, Man, and Cybernetics: Systems*, vol. 47, no. 11, pp. 2994–3005, Nov 2017.
[4] S. Aranovskiy, R. Ortega, J. G. Romero, and D. Sokolov, "A globally exponentially stable speed observer for a class of mechanical systems: experimental and simulation comparison with high-gain and sliding mode designs," *International Journal of Control*, pp. 1–14, 2017. [Online]. Available: https://doi.org/10.1080/00207179.2017.1404130
[5] B. Yi, R. Ortega, and W. Zhang, "On state observers for nonlinear systems: A new design and a unifying framework," *IEEE Transactions on Automatic Control*, vol. 64, no. 3, pp. 1193–1200, March 2019.
[6] S. Battilotti, "Robust observer design under measurement noise with gain adaptation and saturated estimate," *Automatica*, vol. 81, pp. 75–86, 2017.
[7] H. K. Khalil and J. Grizzle, *Nonlinear systems*. Prentice hall New Jersey, 1996.
[8] A. N. Atassi and H. K. Khalil, "A separation principle for the stabilization of a class of nonlinear systems," *IEEE Transactions on Automatic Control*, vol. 44, no. 9, pp. 1672–1687, 1999.
[9] L. Praly and Z. P. Jiang, "Linear output feedback with dynamic high gain for nonlinear systems," *Systems & Control Letters*, vol. 53, pp. 107–116, 2004.

[10] W. He, A. O. David, Z. Yin, and C. Sun, "Neural network control of a robotic manipulator with input deadzone and output constraint," *IEEE Transactions on Systems, Man, and Cybernetics: Systems*, vol. 46, no. 6, pp. 759–770, June 2016.

[11] M. Shakarami, K. Esfandiari, M. A. Shamsi, and M. B. Menhaj, "High-gain observer-based identification scheme for estimation of physical parameters of synchronous generators," in *2016 24th Iranian Conference on Electrical Engineering (ICEE)*, 2016, pp. 1422–1427.

[12] K. Esfandiari, F. Abdollahi, and H. A. Talebi, "Adaptive control of uncertain nonaffine nonlinear systems with input saturation using neural networks," *IEEE Transactions on Neural Networks and Learning Systems*, vol. 26, no. 10, pp. 2311–2322, 2015.

[13] F. Esfandiari and H. K. Khalil, "Output feedback stabilization of fully linearizable systems," *International Journal of Control*, vol. 56, no. 5, pp. 1007–1037, 1992.

[14] D. Astolfi, L. Marconi, L. Praly, and A. Teel, "Sensitivity to high-frequency measurement noise of nonlinear high-gain observers," *IFAC-Papers OnLine*, vol. 49, no. 18, pp. 862–866, 2016.

[15] L. K. Vasiljevica and H. K. Khalil, "Error bounds in differentiation of noisy signals by high-gain observers," *Systems & Control Letters*, vol. 57, no. 10, pp. 856–862, 2001.

[16] H. Kwakernaak and R. Sivan, *Linear Optimal Control Systems*. New York: Wiley-Interscience, 1972.

[17] J. H. Ahrens and H. K. Khalil, "High-gain observers in the presence of measurement noise: A switched-gain approach," *Automatica*, vol. 45, no. 4, pp. 936–943, 2009.

[18] D. Astolfi and L. Marconi, "A high-gain nonlinear observer with limited gain power," *IEEE Transactions on Automatic Control*, vol. 60, no. 11, pp. 3059–3064, 2015.

[19] C. Li, S. Tong, and W. Wang, "Fuzzy adaptive high-gain-based observer backstepping control for siso nonlinear systems," *Information Sciences*, vol. 181, no. 11, pp. 2405–2421, 2011.

[20] C. Ren, S. Tong, and Y. Li, "Fuzzy adaptive high-gain-based observer backstepping control for siso nonlinear systems with dynamical uncertainties," *Nonlinear Dynamics*, vol. 67, no. 2, pp. 941–955, 2012.

[21] K. Esfandiari, F. Abdollahi, and H. A. Talebi, "Adaptive output feedback tracking control for nonaffine nonlinear systems," in *2015 23rd Iranian Conference on Electrical Engineering*. IEEE, 2015, pp. 976–981.

[22] K. S. Narendra and A. Annaswamy, *Stable adaptive systems*. Prentice hall New Jersey, 1989.

[23] K. Esfandiari, F. Abdollahi, and H. A. Talebi, "Adaptive near-optimal neuro controller for continuous-time nonaffine nonlinear systems with constrained input," *Neural Networks*, vol. 93, pp. 195–204, 2017.

[24] K. Esfandiari, F. Abdollahi, and H. A. Talebi, "Stable adaptive output feedback controller for a class of uncertain non-linear systems," *IET Control Theory Applications*, vol. 9, no. 9, pp. 1329–1337, 2015.

[25] M. Shakarami, K. Esfandiari, A. A. Suratgar, and H. A. Talebi, "On the peaking attenuation and transient response improvement of high-gain observers," in *2018 IEEE Conference on Decision and Control (CDC)*, Dec 2018, pp. 577–582.

[26] K. S. Narendra and K. Esfandiari, "Adaptive control of linear periodic systems using multiple models," in *2018 IEEE Conference on Decision and Control (CDC)*, Dec 2018, pp. 589–594.

[27] K. S. Narendra, O. A. Driollet, M. Feiler, and K. George, "Adaptive control using multiple models, switching and tuning," *International Journal of Adaptive Control and Signal Processing*, vol. 17, no. 2, pp. 87–102, 2003.

[28] R. Postoyan, M. H. Hamid, and J. Daafouz, "A multi-observer approach for the state estimation of nonlinear systems," in *2015 54th IEEE Conference on Decision and Control (CDC)*. IEEE, 2015, pp. 1793–1798.

[29] M. S. Chong, D. Nei, R. Postoyan, and L. Kuhlmann, "Parameter and state estimation of nonlinear systems using a multi-observer under the supervisory framework," *IEEE Transactions on Automatic Control*, vol. 60, no. 9, pp. 2336–2349, 2015.

[30] Z. Han and K. S. Narendra, "New concepts in adaptive control using multiple models," *IEEE Transactions on Automatic Control*, vol. 57, no. 1, p. 7889, 2012.

[31] I. J. Bakelman, *Convex analysis and nonlinear geometric elliptic equations*. Springer Science & Business Media, 2012.

[32] W. Wang, Y. Chien, and T. Lee, "Observer-based t-s fuzzy control for a class of general nonaffine nonlinear systems using generalized projection-update laws," *IEEE Transactions on Fuzzy Systems*, vol. 19, no. 3, pp. 493–504, 2011.

Kasra Esfandiari (S'13) received the B.Sc. degree in electrical engineering/control systems from Shiraz University, Shiraz, Iran, in 2012, and the M.Sc. degree in electrical engineering/control systems from the Amirkabir University of Technology, Tehran, Iran, in 2014. In 2018, he received his second M.Sc. degree in electrical engineering from Yale University, New Haven, USA, where he is currently a Ph.D. candidate. His current research interests include adaptive control, neural networks, nonlinear control, fault diagnosis and recovery, and robotics.

Mehran Shakarami received the M.Sc. degree in electrical engineering from Amirkabir University of Technology (Tehran polytechnic), Tehran, Iran, in 2014, and B.Sc. and A.Sc. degrees from Shamsipour College, Tehran, Iran, in 2011 and 2009, respectively. He is currently a Ph.D. student at the University of Groningen, Groningen, The Netherlands, and his current research interests include dynamical networks, game theory, nonlinear control, adaptive control, robust control, and system identification.